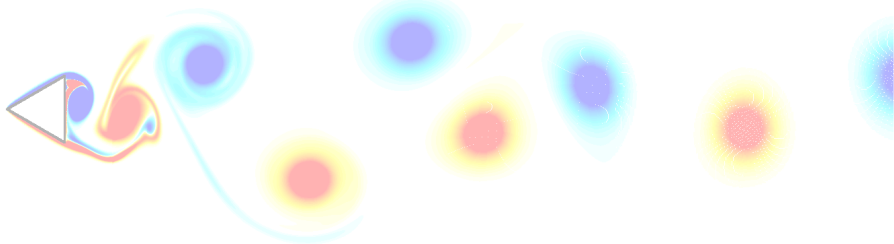


# Chorin's approaches revisited: Particle Vortex Method vs Finite Volume Method

Giannopoulou Ourania

Advisors: Colagrossi A. (CNR - INM), Di Mascio A. (Uni. L' Aquila)

Seminario di Modellistica Differenziale Numerica  
Sapienza Department of Mathematics  
26.02.2019



## Introduction

### Splitting approach and projection method for NSE

- Solving NSE in  $\omega - u$

  - Representation of potential flow through an IBEM
  - Evaluation of hydrodynamic loads

- Solving NSE in  $u - p$

### Brief description on the numerical schemes adopted

- The Diffused Vortex Hydrodynamics (Particle Vortex Method)

  - The advection step

  - The diffusion step

- The Finite Volume Method

### Comparison between FVM and DVH method through benchmark tests

- Flow past a circular cylinder in an unsteady current

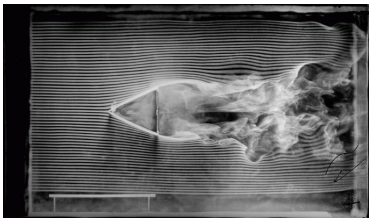
- Flow around an ellipse with incidence

- Flow around a cylinder with triangular section

## Conclusions

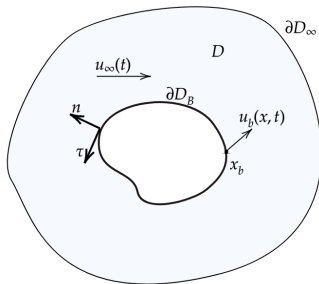
# Introduction

# Statement of the problem



$$\begin{cases} \frac{D\mathbf{u}}{Dt} = -\frac{\nabla p}{\rho_0} + \nu \nabla^2 \mathbf{u} + \mathbf{f} \\ \nabla \cdot \mathbf{u} = 0 \end{cases} \quad \mathbf{x} \in D$$

$$\begin{cases} \mathbf{u}(\mathbf{x}, 0) = \mathbf{u}_0(\mathbf{x}) & \mathbf{x} \in D, \\ \mathbf{u}(\mathbf{x}_b) = \mathbf{u}_b & \mathbf{x} \in \partial D_B, \\ \mathbf{u}(\mathbf{x}, t) \rightarrow \mathbf{u}_\infty(t) & |\mathbf{x}| \rightarrow \infty, \end{cases}$$



# Splitting approach and projection method for NSE

Vorticity formulation of NS for incompressible fluid:

$$\left. \begin{array}{l} \nabla \times \left( \frac{D\mathbf{u}}{Dt} = -\frac{\nabla p}{\rho} + \nu \nabla^2 \mathbf{u} \right) \\ \omega = \nabla \times \mathbf{u} \quad \nabla \cdot \mathbf{u} = 0 \end{array} \right\} \Rightarrow \frac{D\omega}{Dt} = \omega \cdot \nabla \mathbf{u} + \nu \nabla^2 \omega,$$

Vorticity formulation of NS for incompressible fluid:

$$\left. \begin{array}{l} \nabla \times \left( \frac{D\mathbf{u}}{Dt} = -\frac{\nabla p}{\rho} + \nu \nabla^2 \mathbf{u} \right) \\ \omega = \nabla \times \mathbf{u} \quad \nabla \cdot \mathbf{u} = 0 \end{array} \right\} \Rightarrow \frac{D\omega}{Dt} = \omega \cdot \nabla \mathbf{u} + \nu \nabla^2 \omega,$$

- ▶ in 2D the stretching term  $\omega \cdot \nabla \mathbf{u}$  is zero

$$\left\{ \begin{array}{ll} \frac{D\omega}{Dt} &= \nu \nabla^2 \omega, \quad \text{on } D, \\ \omega(\mathbf{x}, 0) &= \omega_0(\mathbf{x}), \quad \text{for all } \mathbf{x} \in D, \end{array} \right.$$

Vorticity formulation of NS for incompressible fluid:

$$\left. \begin{aligned} \nabla \times \left( \frac{D\mathbf{u}}{Dt} = -\frac{\nabla p}{\rho} + \nu \nabla^2 \mathbf{u} \right) \\ \omega = \nabla \times \mathbf{u} \quad \nabla \cdot \mathbf{u} = 0 \end{aligned} \right\} \Rightarrow \frac{D\omega}{Dt} = \omega \cdot \nabla \mathbf{u} + \nu \nabla^2 \omega,$$

- in 2D the stretching term  $\omega \cdot \nabla \mathbf{u}$  is zero

$$\left\{ \begin{aligned} \frac{D\omega}{Dt} &= \nu \nabla^2 \omega, \quad \text{on } D, \\ \omega(\mathbf{x}, 0) &= \omega_0(\mathbf{x}), \quad \text{for all } \mathbf{x} \in D, \end{aligned} \right.$$

- Use Operator Splitting to get the two sub-problems of advection and diffusion

$$\begin{aligned} \text{ADVECTION} \quad & \left\{ \begin{aligned} \frac{D\omega}{Dt} &= 0, \\ \frac{D\mathbf{x}}{Dt} &= \mathbf{u}(\mathbf{x}, t), \end{aligned} \right. & \nabla^2 \mathbf{u} &= -\nabla \times \omega \\ \text{DIFFUSION} \quad & \left\{ \begin{aligned} \partial_t \omega &= \nu \nabla^2 \omega, \quad \text{in } D \\ \nu \frac{\partial \omega}{\partial n} &= -\dot{\gamma}, \quad \text{on } \partial D_B \end{aligned} \right. \end{aligned}$$

## Representation of potential flow through an IBEM ( $\omega - u$ )

$$ADVECTION \quad \left\{ \begin{array}{l} \frac{D\omega}{Dt} = 0, \\ \frac{D\mathbf{x}}{Dt} = \mathbf{u}(\mathbf{x}, t), \end{array} \right. \quad \nabla^2 \mathbf{u} = -\nabla \times \omega,$$

- Decompose velocity field using Helmholtz-Hodge decomposition

$$\mathbf{u}(\mathbf{x}, t) = \nabla\phi + \nabla \times \boldsymbol{\psi} = \mathbf{u}_\infty(t) + \mathbf{u}_\phi(\mathbf{x}, t) + \mathbf{u}_\omega(\mathbf{x}, t),$$

- Assign the rotational part to  $\mathbf{u}_\omega$  where

$$\mathbf{u}_\omega = \int_D K(\mathbf{x}, \mathbf{y}) \omega(\mathbf{y}) d\mathbf{y}$$

- Represent irrotational part through an IBEM and use it to enforce the no-slip BCs

$$\mathbf{u}_\phi(\mathbf{x}, t) = - \int_{\partial D_B} \boxed{\sigma(\mathbf{y}, t)} \nabla G(\mathbf{x}, \mathbf{y}) d\mathbf{l}_y + \int_{\partial D_B} \boxed{\gamma(\mathbf{y}, t)} \mathbf{K}(\mathbf{x}, \mathbf{y}) d\mathbf{l}_y,$$

Unknown source density                      Unknown circulation density

where  $G(\mathbf{x}, \mathbf{y}) = -\frac{1}{2\pi} \log(|\mathbf{x} - \mathbf{y}|)$ ,  $K(\mathbf{x}, \mathbf{y}) = \nabla \times (G\mathbf{e}_3)$  are in free space

## Representation of potential flow through an IBEM ( $\omega - u$ )

---

### Evaluation of $\sigma$ :

- Assign a constant density circulation

$$\gamma(\mathbf{y}, t) = \hat{\gamma}(t) = -\Gamma(t)/\mathcal{P}, \quad \Gamma(t) = \int_D \omega(\mathbf{y}, t) d\mathbf{y}.$$

- this leads to

$$\mathbf{u}'_{\phi}(\mathbf{x}, t) = - \int_{\partial D_B} \sigma(\mathbf{y}, t) \nabla G(\mathbf{x}, \mathbf{y}) dl_y + \hat{\gamma}(t) \int_{\partial D_B} \mathbf{K}(\mathbf{x}, \mathbf{y}) dl_y,$$

## Representation of potential flow through an IBEM ( $\omega - u$ )

### Evaluation of $\sigma$ :

- Assign a constant density circulation

$$\gamma(\mathbf{y}, t) = \hat{\gamma}(t) = -\Gamma(t)/\mathcal{P}, \quad \Gamma(t) = \int_D \omega(\mathbf{y}, t) d\mathbf{y}.$$

- this leads to

$$\mathbf{u}'_{\phi}(\mathbf{x}, t) = - \int_{\partial D_B} \sigma(\mathbf{y}, t) \nabla G(\mathbf{x}, \mathbf{y}) dl_y + \hat{\gamma}(t) \int_{\partial D_B} \mathbf{K}(\mathbf{x}, \mathbf{y}) dl_y,$$

- Apply no through condition for potential flow to find  $\sigma$

$$(\mathbf{u}'_{\phi} \cdot \mathbf{n})(s, t) = [\mathbf{u}_b(s, t) - \mathbf{u}_{\infty}(t)] \cdot \mathbf{n}(s, t) - \mathbf{u}_{\omega}(s, t) \cdot \mathbf{n}(s, t), \quad s \in \partial D_B.$$

## Representation of potential flow through an IBEM ( $\omega - u$ )

### Evaluation of $\sigma$ :

- Assign a constant density circulation

$$\gamma(\mathbf{y}, t) = \hat{\gamma}(t) = -\Gamma(t)/\mathcal{P}, \quad \Gamma(t) = \int_D \omega(\mathbf{y}, t) d\mathbf{y}.$$

- this leads to

$$\mathbf{u}'_{\phi}(\mathbf{x}, t) = - \int_{\partial D_B} \sigma(\mathbf{y}, t) \nabla G(\mathbf{x}, \mathbf{y}) dl_y + \hat{\gamma}(t) \int_{\partial D_B} \mathbf{K}(\mathbf{x}, \mathbf{y}) dl_y,$$

- Apply no through condition for potential flow to find  $\sigma$

$$(\mathbf{u}'_{\phi} \cdot \mathbf{n})(s, t) = [\mathbf{u}_b(s, t) - \mathbf{u}_{\infty}(t)] \cdot \mathbf{n}(s, t) - \mathbf{u}_{\omega}(s, t) \cdot \mathbf{n}(s, t), \quad s \in \partial D_B.$$

- Discretize the boundary into  $N$  panels with constant strength  $\hat{\gamma}$ :

$$[\mathbf{A}]\{\sigma\} = [\mathbf{C}]\{\hat{\gamma}\} - \{\mathbf{u}_b \cdot \mathbf{n}\} + \{\mathbf{u}_{\infty} \cdot \mathbf{n}\} + \{\mathbf{u}_{\omega} \cdot \mathbf{n}\}$$

- Solve the  $N \times N$  system to get  $\sigma$  using *LDU decomposition*

## Representation of potential flow through an IBEM ( $\omega - u$ )

---

### Evaluation of $\gamma$ :

- Generation of circulation density to enforce no-slip BC

$$\gamma(s, t) = [\mathbf{u}_b(s, t) - \mathbf{u}_\infty(t)] \cdot \boldsymbol{\tau}(s, t) - [\mathbf{u}'_\phi(s, t) + \mathbf{u}_\omega(s, t)] \cdot \boldsymbol{\tau}(s, t), \quad s \in \partial D_B,$$

- The discretized form is

$$\{\gamma\} = [\mathbf{A}]\{\hat{\gamma}\} + [\mathbf{C}]\{\sigma\} - \{\mathbf{u}_b \cdot \mathbf{n}\} + \{\mathbf{u}_\infty \cdot \mathbf{n}\} + \{\mathbf{u}_\omega \cdot \mathbf{n}\}$$

$\gamma$  is diffused during the diffusion step into the flow using the Neumann bc

## Representation of potential flow through an IBEM ( $\omega - u$ )

---

### Evaluation of $\gamma$ :

- Generation of circulation density to enforce no-slip BC

$$\gamma(s, t) = [\mathbf{u}_b(s, t) - \mathbf{u}_\infty(t)] \cdot \boldsymbol{\tau}(s, t) - [\mathbf{u}'_\phi(s, t) + \mathbf{u}_\omega(s, t)] \cdot \boldsymbol{\tau}(s, t), \quad s \in \partial D_B,$$

- The discretized form is

$$\{\gamma\} = [\mathbf{A}]\{\hat{\gamma}\} + [\mathbf{C}]\{\sigma\} - \{\mathbf{u}_b \cdot \mathbf{n}\} + \{\mathbf{u}_\infty \cdot \mathbf{n}\} + \{\mathbf{u}_\omega \cdot \mathbf{n}\}$$

$\gamma$  is diffused during the diffusion step into the flow using the Neumann bc

$$\mathbf{u}_\phi(\mathbf{x}, t) = - \int_{\partial D_B} \sigma(\mathbf{y}, t) \nabla G(\mathbf{x}, \mathbf{y}) d\mathbf{y} + \int_{\partial D_B} \gamma(\mathbf{y}, t) \mathbf{K}(\mathbf{x}, \mathbf{y}) d\mathbf{y},$$

# Representation of potential flow through an IBEM ( $\omega - u$ )

## Evaluation of $\gamma$ :

- Generation of circulation density to enforce no-slip BC

$$\gamma(s, t) = [\mathbf{u}_b(s, t) - \mathbf{u}_\infty(t)] \cdot \boldsymbol{\tau}(s, t) - [\mathbf{u}'_\phi(s, t) + \mathbf{u}_\omega(s, t)] \cdot \boldsymbol{\tau}(s, t), \quad s \in \partial D_B,$$

- The discretized form is

$$\{\gamma\} = [\mathbf{A}]\{\hat{\gamma}\} + [\mathbf{C}]\{\sigma\} - \{\mathbf{u}_b \cdot \mathbf{n}\} + \{\mathbf{u}_\infty \cdot \mathbf{n}\} + \{\mathbf{u}_\omega \cdot \mathbf{n}\}$$

$\gamma$  is diffused during the diffusion step into the flow using the Neumann bc

$$\mathbf{u}_\phi(\mathbf{x}, t) = - \int_{\partial D_B} \sigma(\mathbf{y}, t) \nabla G(\mathbf{x}, \mathbf{y}) d\mathbf{y} + \int_{\partial D_B} \gamma(\mathbf{y}, t) \mathbf{K}(\mathbf{x}, \mathbf{y}) d\mathbf{y},$$

- Particles are advected during the next advection step with velocity that satisfies the no-slip BC

$$\mathbf{u}(\mathbf{x}, t) = \mathbf{u}_\infty(t) + \int_{\partial D_B} \left[ \mathbf{K}(\mathbf{x}, \mathbf{y}) \gamma(\mathbf{y}) - \mathbf{e}_3 \times \mathbf{K}(\mathbf{x}, \mathbf{y}) \sigma(\mathbf{y}) \right] d\mathbf{y} + \int_D \mathbf{K}(\mathbf{x}, \mathbf{y}) \omega(\mathbf{y}) d\mathbf{y}.$$

# Evaluation of hydrodynamic loads ( $\omega - u$ )

- Total force: Drag and Lift coefficients

$$\mathbf{F}_B = \int_{\partial D_B} (-p\mathbf{n} + \mu\omega\boldsymbol{\tau}) \rightarrow \begin{cases} C_D = \frac{F_{B_x}}{\frac{1}{2}\rho u_\infty^2 S} \\ C_L = \frac{F_{B_y}}{\frac{1}{2}\rho u_\infty^2 S}, \end{cases}$$

- Torque around the center of mass  $\mathbf{x}_{cm}$

$$\mathbf{T}_B = \int_{\partial D_B} (\mathbf{x} - \mathbf{x}_{cm}) \times (-p\mathbf{n} + \mu\omega\boldsymbol{\tau}),$$

- Pressure

$$\frac{1}{\rho_0} \frac{\partial p}{\partial s} = \boldsymbol{\tau}(s) \cdot [\dot{\mathbf{u}}_\infty - \dot{\mathbf{u}}_b(s)] + \dot{\gamma}(s), \quad s \in \partial D_B.$$

- Apply the divergence operator on NSE

$$\frac{D}{Dt}(\nabla \cdot \mathbf{u}) - \omega^2 + \nabla \mathbf{u} : \nabla \mathbf{u} = -\frac{\nabla^2 p}{\rho_0} + \nu \nabla^2(\nabla \cdot \mathbf{u}),$$

## Method 1

- Use incompressibility condition to get a Pressure Poisson equation

$$\begin{cases} \nabla^2 p = \rho_0 (\omega^2 - \nabla \mathbf{u} : \nabla \mathbf{u}), \\ \frac{\partial p}{\partial n} = -\mathbf{n} \cdot [\dot{\mathbf{u}}_b - \dot{\mathbf{u}}_\infty] + \nu \frac{\partial \omega}{\partial \tau}, \quad \text{on } \partial D_B, \end{cases}$$

## Main drawback

- The method does not guarantee divergence free flow field, because

$$\begin{aligned} \frac{D}{Dt}(\nabla \cdot \mathbf{u}) &= \nu \nabla^2(\nabla \cdot \mathbf{u}), \\ \nabla \cdot \mathbf{u} \Big|_{t=0} &= 0, \end{aligned}$$

- If incompressibility is not satisfied at  $t = 0$  or on the boundary, then  $\nabla \cdot \mathbf{u} \neq 0$  in the field

## Method 2

- Evaluate velocity from momentum equation ignoring viscous contributions and the divergence constraint

$$\mathbf{u}^* = \mathbf{u}^n + \nu \nabla^2 \mathbf{u}^n \Delta t.$$

- Decompose resulting velocity using Helmholtz - Hodge decomposition (HHD)

$$\mathbf{u}^* = \nabla \times \Psi + \nabla \Phi.$$

- Assign the rotational part to the velocity at next level and the irrotational to the pressure gradient

$$\nabla \times \Psi = \mathbf{u}^{n+1}, \quad \nabla \Phi = \left( \frac{\nabla p}{\rho_0} \right)^{n+1} \Delta t.$$

- The velocity at next level is divergent free

$$\mathbf{u}^{n+1} = \mathbf{u}^* - \left( \frac{\nabla p}{\rho_0} \right)^{n+1} \Delta t$$

- Apply divergence operator

$$\nabla^2 p^{n+1} = \rho_0 \frac{(\nabla \cdot \mathbf{u}^*)}{\Delta t}.$$

## Method 3

- ▶ The divergence constraint is coupled to the momentum equation by introducing the pressure field

$$\begin{cases} \frac{\partial \mathbf{u}}{\partial \tau} + \frac{D\mathbf{u}}{Dt} = -\frac{\nabla p}{\rho_0} + \nu \nabla^2 \mathbf{u}, \\ \frac{\partial p}{\partial \tau} + \beta \nabla \cdot \mathbf{u} = 0, \end{cases}$$

where  $\beta$ : pseudo-compressibility parameter,  $\tau$ : pseudo-time,  $\sqrt{\beta}$ : pseudo-sound speed

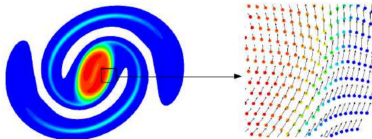
- ▶ Use Dual Time Stepping
- ▶ At each iteration in real time we do sub-iterations in pseudo-time to enforce incompressibility
- ▶ Obtain a solution that satisfies  $\nabla \cdot \mathbf{u}$  when steady state is reached in  $\tau$

# **Brief description on the numerical schemes adopted**

# Diffused Vortex Hydrodynamics: The advection step

- Discretization of vorticity field

$$\omega_\epsilon(\mathbf{x}, t) \approx \sum_{j=1}^{N_v} \Gamma_j(t) \delta_\epsilon(\mathbf{x} - \mathbf{x}_j(t))$$



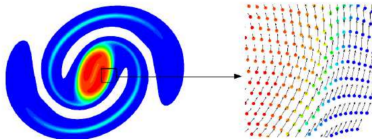
- Evaluation of velocity that satisfies no - slip condition

$$\mathbf{u}(\mathbf{x}_i, t) = \mathbf{u}_\infty(t) + \underbrace{\sum_{k=1}^{N_b} [\mathbf{K}_\epsilon(\mathbf{x}_i, \mathbf{y}_k) \gamma_k(t) - \mathbf{e}_3 \times \mathbf{K}_\epsilon(\mathbf{x}_i, \mathbf{y}_k) \sigma_k(t)] \Delta s}_{\mathbf{u}_\phi(t)} + \underbrace{\sum_{j=1}^{N_v} \Gamma_j(t) \mathbf{K}_\epsilon(\mathbf{x}_i, \mathbf{y}_j)}_{\mathbf{u}_\omega(t)}$$

# Diffused Vortex Hydrodynamics: The advection step

- Discretization of vorticity field

$$\omega_\epsilon(\mathbf{x}, t) \approx \sum_{j=1}^{N_v} \Gamma_j(t) \delta_\epsilon(\mathbf{x} - \mathbf{x}_j(t))$$



- Evaluation of velocity that satisfies no - slip condition

$$\mathbf{u}(\mathbf{x}_i, t) = \mathbf{u}_\infty(t) + \underbrace{\sum_{k=1}^{N_b} [\mathbf{K}_\epsilon(\mathbf{x}_i, \mathbf{y}_k) \gamma_k(t) - \mathbf{e}_3 \times \mathbf{K}_\epsilon(\mathbf{x}_i, \mathbf{y}_k) \sigma_k(t)] \Delta s}_{\mathbf{u}_\phi(t)} + \underbrace{\sum_{j=1}^{N_v} \Gamma_j(t) \mathbf{K}_\epsilon(\mathbf{x}_i, \mathbf{y}_j)}_{\mathbf{u}_\omega(t)}$$

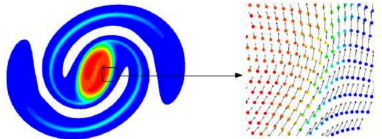
- Advect particles using 4<sup>th</sup> order Runge - Kutta

$$\begin{cases} \frac{d\mathbf{x}_i(t)}{dt} = \mathbf{u}(\mathbf{x}_i, t) \\ \frac{D\Gamma_i(t)}{Dt} = 0 \end{cases}$$

# Diffused Vortex Hydrodynamics: The advection step

- Discretization of vorticity field

$$\omega_\epsilon(\mathbf{x}, t) \approx \sum_{j=1}^{N_v} \Gamma_j(t) \delta_\epsilon(\mathbf{x} - \mathbf{x}_j(t))$$



- Evaluation of velocity that satisfies no - slip condition

$$\mathbf{u}(\mathbf{x}_i, t) = \mathbf{u}_\infty(t) + \underbrace{\sum_{k=1}^{N_b} [\mathbf{K}_\epsilon(\mathbf{x}_i, \mathbf{y}_k) \gamma_k(t) - \mathbf{e}_3 \times \mathbf{K}_\epsilon(\mathbf{x}_i, \mathbf{y}_k) \sigma_k(t)] \Delta s}_{\mathbf{u}_\phi(t)} + \underbrace{\sum_{j=1}^{N_v} \Gamma_j(t) \mathbf{K}_\epsilon(\mathbf{x}_i, \mathbf{y}_j)}_{\mathbf{u}_\omega(t)}$$

- Advect particles using 4<sup>th</sup> order Runge - Kutta

$$\begin{cases} \frac{d\mathbf{x}_i(t)}{dt} = \mathbf{u}(\mathbf{x}_i, t) \\ \frac{D\Gamma_i(t)}{Dt} = 0 \end{cases}$$

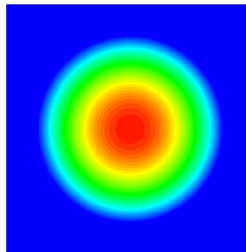
## Advection Time step

$$\Delta t_a = K_a \frac{\Delta r_{min}}{U}$$

$K_a \sim O(10^{-1})$

$\Delta r_{min}$ : size of the smallest particle

$U$ : reference velocity



- Diffusion is performed in deterministic way
- Truncate the exact solution of the heat equation within  $R_d$  (diffusive radius).
- Then *each particle* diffuses according to

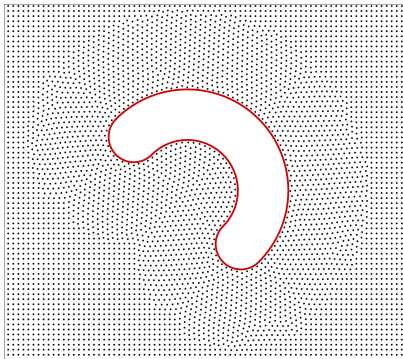
$$\omega(\mathbf{x}, t + \Delta t) = \begin{cases} \frac{\Gamma_i}{4\pi\nu\Delta t_d} \exp\left(-\frac{|\mathbf{x} - \mathbf{x}_i|^2}{4\nu\Delta t_d}\right) & |\mathbf{x} - \mathbf{x}_i| \leq R_d, \\ 0 & \text{otherwise,} \end{cases}$$

- The truncation introduces a relative error of circulation conservation:

$$\xi = \exp\left(-\frac{R_d^2}{4\nu\Delta t_d}\right).$$

- To respect the conservation of circulation a redistribution procedure is performed

# Packing Algorithm



- Generates a body fitted distribution of points around the boundary



Allows to model flows around arbitrary geometries without the need of generating a mesh

- The distribution of particles is regular (all particles have a uniform mean distance)

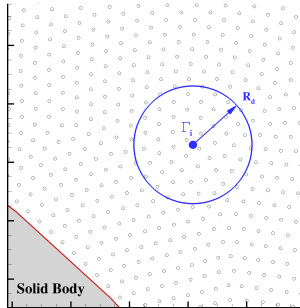


Can be used to address the problem of Lagrangian distortion

- We call this distribution *Regular Point Distribution (RPD)*

# Diffused Vortex Hydrodynamics: The Diffusion step

- Diffusion of a vortex is performed on a Regular Point Distribution (RPD)

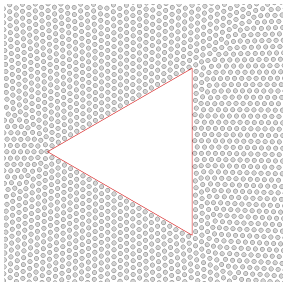


- Start with a single point vortex
- Find the points with  $|x - x_0| \leq R_d$
- Use approx. solution of heat eq. to diffuse circulation over the nodes
- Conserve circulation with a redistribution procedure
- The nodes of the RPD become the new vortices

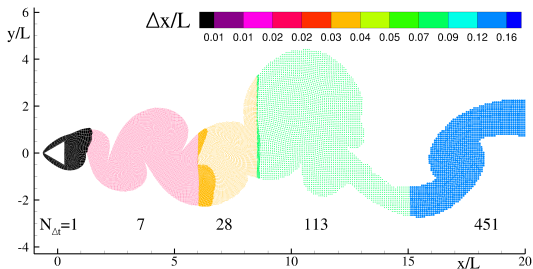
## Diffusion Time step

$$\Delta t_d = 0.021 \frac{R_d^2}{\nu} = 0.34 \frac{\Delta r_j^2}{\nu}$$

# Adaptive Particle Refinement



- ▶ Close to the body we have the finest resolution (small particles)
- ▶ Far from the body the resolution in decreased
- ▶ In this way we contain the growth of particles during diffusion



- The computational domain  $D$  is split into subdomains, each discretized by a block-structured grid subdivided into  $N_i \times N_j$  subdomains  $D_{ij}$ . The NSEs are written in integral form on each volume  $D_{ij}$ :

$$\left\{ \begin{array}{l} \int_{\partial D_{ij}} \mathbf{u} \cdot \mathbf{n} dS = 0, \\ \int_{D_{ij}} \frac{\partial \mathbf{u}}{\partial t} dV + \int_{\partial D_{ij}} \mathbf{F} \cdot \mathbf{n} dS = 0, \end{array} \right.$$

$$\mathbf{F} = \mathbf{u} \otimes \mathbf{u} + \frac{p}{\rho_0} \mathbb{I} - \mathbb{T}$$

$$\mathbb{T} = \nu (\nabla \mathbf{u} + \nabla^T \mathbf{u}),$$

$\mathbb{I}$ : unit tensor,  $\mathbb{T}$ : stress tensor.

- The computational domain  $D$  is split into subdomains, each discretized by a block-structured grid subdivided into  $N_i \times N_j$  subdomains  $D_{ij}$ . The NSEs are written in integral form on each volume  $D_{ij}$ :

$$\left\{ \begin{array}{l} \int_{\partial D_{ij}} \mathbf{u} \cdot \mathbf{n} dS = 0, \\ \int_{D_{ij}} \frac{\partial \mathbf{u}}{\partial t} dV + \int_{\partial D_{ij}} \mathbf{F} \cdot \mathbf{n} dS = 0, \end{array} \right.$$

Setting:

$$\mathbf{u}_{ij} = \frac{1}{V_{ij}} \int_{D_{ij}} \mathbf{u} dV,$$

$$\mathbf{F}_I = \int_{S_I} \mathbf{F} \cdot \mathbf{n} dS,$$

$$\mathbf{U}_I = \int_{S_I} \mathbf{u} \cdot \mathbf{n} dS,$$

$$\mathbf{F} = \mathbf{u} \otimes \mathbf{u} + \frac{p}{\rho_0} \mathbb{I} - \mathbb{T}$$

$$\mathbb{T} = \nu (\nabla \mathbf{u} + \nabla^T \mathbf{u}),$$

$\mathbb{I}$ : unit tensor,  $\mathbb{T}$ : stress tensor.

- The computational domain  $D$  is split into subdomains, each discretized by a block-structured grid subdivided into  $N_i \times N_j$  subdomains  $D_{ij}$ . The NSEs are written in integral form on each volume  $D_{ij}$ :

$$\left\{ \begin{array}{l} \int_{\partial D_{ij}} \mathbf{u} \cdot \mathbf{n} dS = 0, \\ \int_{D_{ij}} \frac{\partial \mathbf{u}}{\partial t} dV + \int_{\partial D_{ij}} \mathbf{F} \cdot \mathbf{n} dS = 0, \end{array} \right.$$

Setting:

$$\mathbf{u}_{ij} = \frac{1}{V_{ij}} \int_{D_{ij}} \mathbf{u} dV,$$

$$\mathbf{F}_l = \int_{S_l} \mathbf{F} \cdot \mathbf{n} dS,$$

$$\mathbf{U}_l = \int_{S_l} \mathbf{u} \cdot \mathbf{n} dS,$$

$$\mathbf{F} = \mathbf{u} \otimes \mathbf{u} + \frac{p}{\rho_0} \mathbb{I} - \mathbb{T}$$

$$\mathbb{T} = \nu (\nabla \mathbf{u} + \nabla^T \mathbf{u}),$$

$\mathbb{I}$ : unit tensor,  $\mathbb{T}$ : stress tensor.

$$\left\{ \begin{array}{l} \sum_{l \in L_{ij}} \mathbf{U}_l = 0, \\ V_{ij} \frac{d\mathbf{u}_{ij}}{dt} + \sum_{l \in L_{ij}} \mathbf{F}_l = 0, \end{array} \right.$$

- $L_{ij}$  is the subset of the cell interfaces for subdomain  $D_{ij}$ .

- Implicit Crank Nicolson in time

$$\begin{cases} \sum_{l \in L_{ij}} \mathbf{u}_l^{n+1} = 0, \\ V_{ij} \frac{\mathbf{v}_{ij}^{n+1} - \mathbf{v}_{ij}^n}{\Delta t} + \frac{1}{2} \left( \sum_{l \in L_{ij}} \mathbf{F}_l^{n+1} + \sum_{l \in L_{ij}} \mathbf{F}_l^n \right) = 0, \end{cases}$$

- Pseudo-Compressibility in pseudo-time

$$\begin{cases} \frac{\partial p^{n+1}}{\partial \tau} + \rho_0 \beta \left( \sum_{l \in L_{ij}} \mathbf{u}_l^{n+1} \right) = 0, \\ \frac{\partial \mathbf{v}^{n+1}}{\partial \tau} + \left[ V_{ij} \frac{\mathbf{v}_{ij}^{n+1} - \mathbf{v}_{ij}^n}{\Delta t} + \frac{1}{2} \left( \sum_{l \in L_{ij}} \mathbf{F}_l^{n+1} + \sum_{l \in L_{ij}} \mathbf{F}_l^n \right) \right] = 0. \end{cases}$$

# FVM: Grid structure

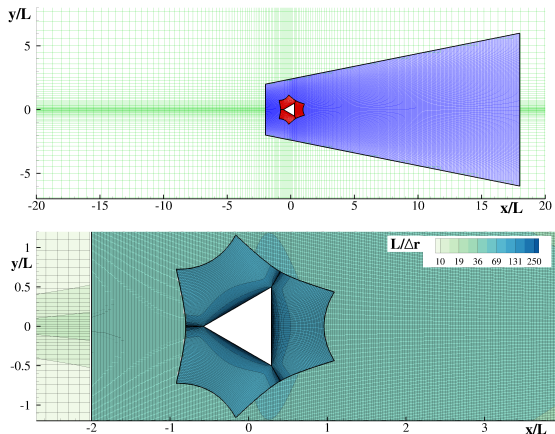


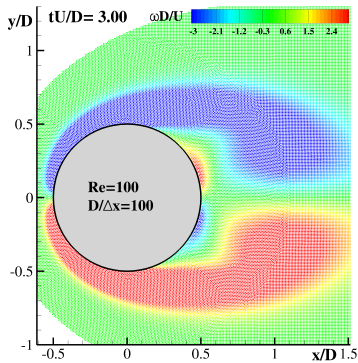
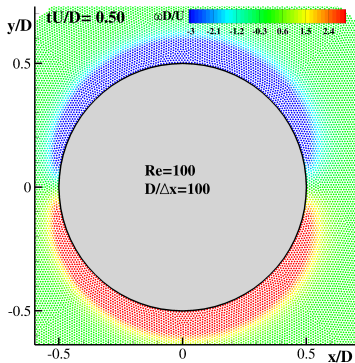
**Figure:** Discretization of the computational domain used for the FVM. Top: fluid domain from  $-20L$  to  $20L$  to enforce the radiation condition for the pressure; the three chimera blocks in different colors. Bottom: view around the solid body; the color is representative of the local spatial resolution  $L/\Delta r$ , where  $\Delta r$  is the square root of the cell volume.

# Comparison between FVM and DVH method through benchmark tests

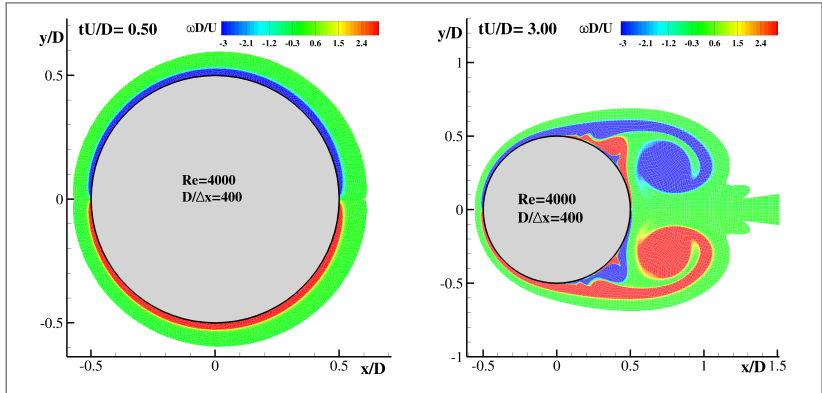
# Flow past a circular cylinder in an unsteady current

$$u_{\infty}(t) = \begin{cases} \frac{U}{2} \left[ 1 - \cos \left( \frac{\pi t}{t_r} \right) \right] & t \leq t_r \\ U & t > t_r \end{cases}$$

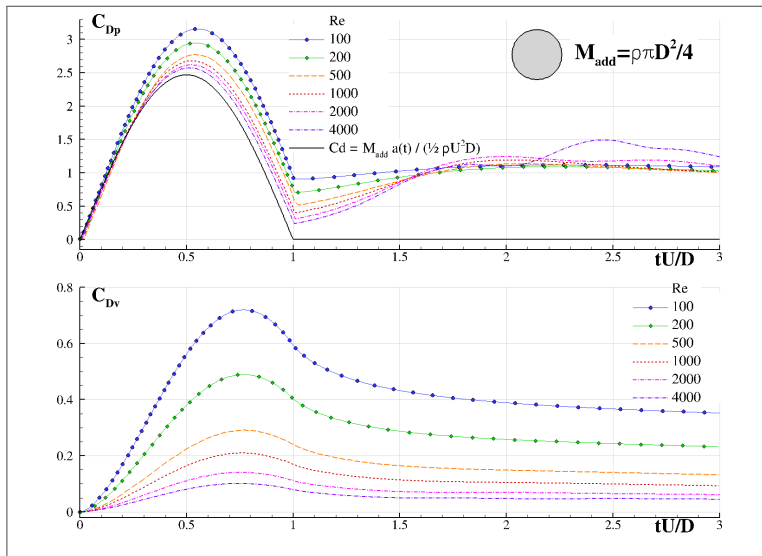
$$C_{Dp} = \frac{\int_{\partial D_B} -pn \cdot \mathbf{e}_1 ds}{\frac{1}{2} \rho U^2 D}, \quad C_{Dv} = \frac{\int_{\partial D_B} \mu \omega \tau \cdot \mathbf{e}_1 ds}{\frac{1}{2} \rho U^2 D}$$



# Flow past a circular cylinder in an unsteady current

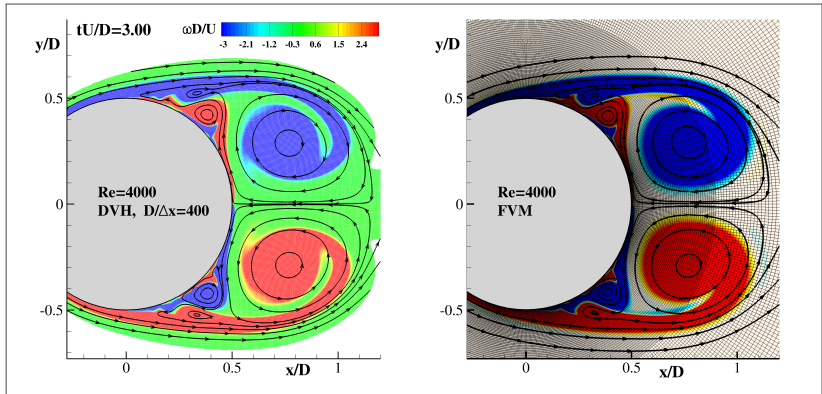


# Flow past a circular cylinder in an unsteady current



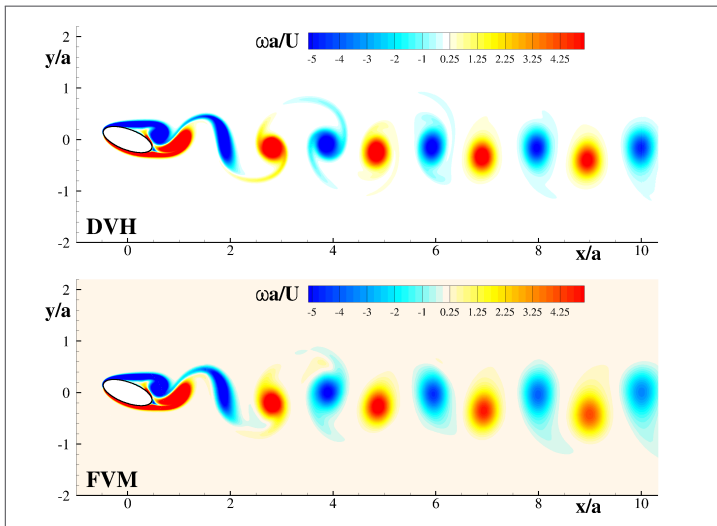
# Flow past a circular cylinder in an unsteady current

Comparison with FVM for  $Re = 4000$



# Flow around an ellipse with incidence

Vorticity Fields,  $Re = 1000$

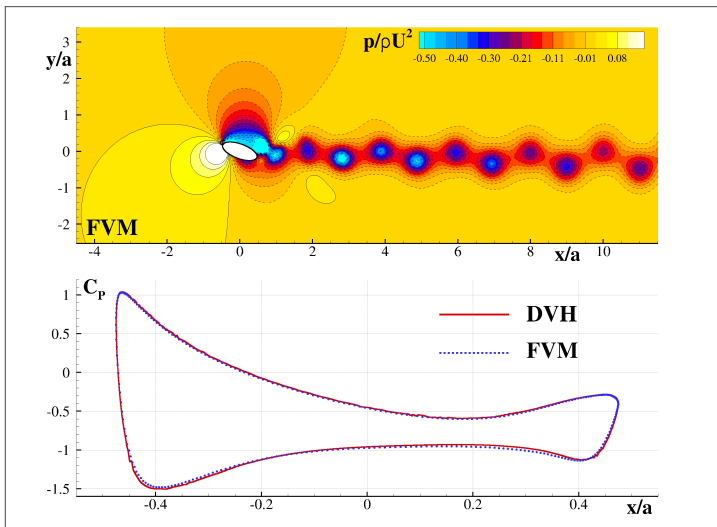


AoA:  $\alpha = 20^\circ$

Axis ratio :  $b/a = 0.4$

# Flow around an ellipse with incidence

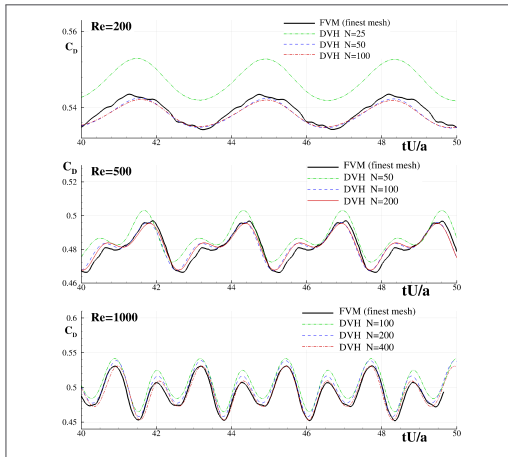
Comparison with FVM for  $Re = 1000$ , Pressure coeff.



Pressure coefficient:  $C_p = \frac{(p - p_\infty)}{\frac{1}{2} \rho U^2}$

# Flow around an ellipse with incidence

Comparison with FVM for  $Re = 200, 500, 1000$ . Convergence results



$$\epsilon_{21} = \int_{t_0}^{t_f} |f_2 - f_1| dt$$

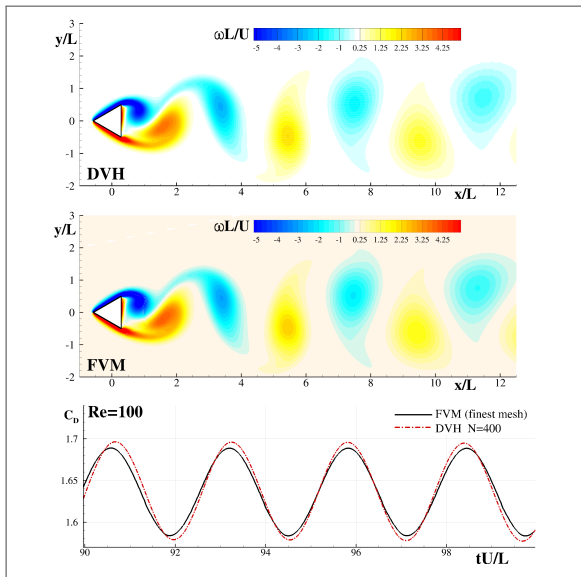
Convergence rate

$$C(C_D) = \log\left(\frac{\epsilon_{32}}{\epsilon_{21}}\right) / \log(2)$$

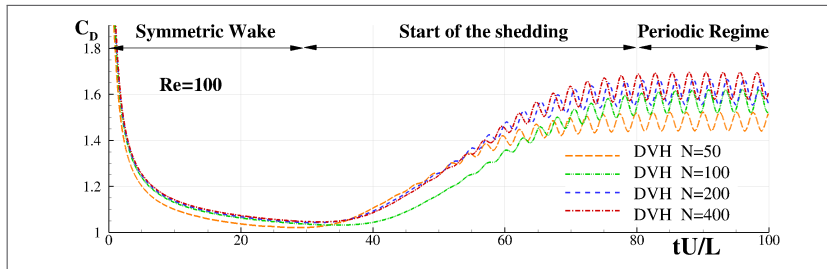
Re	$C(C_D)$	
	DVH	FVM
200	4.1	4.2
500	2.7	4.1
1000	2.0	2.4

# Flow around a cylinder with triangular section $Re=100$

## Vorticity fields and forces



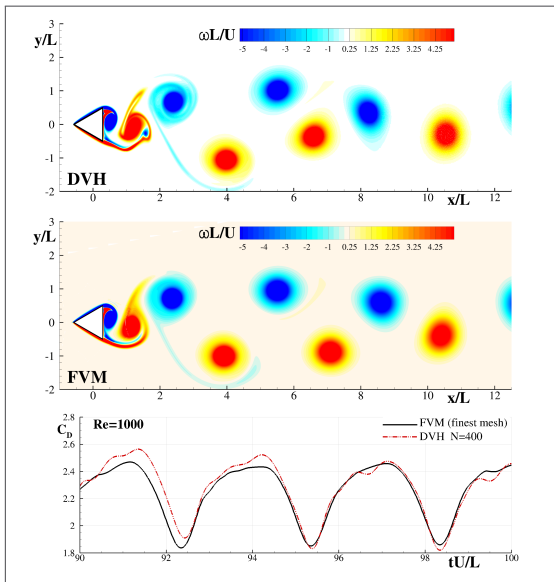
# Flow around a cylinder with triangular section $Re=100$



	$C(C_D)$	
	$tU/L \in [0, 30]$	$tU/L > 30$
DVH	2.0	1.0
FVM	2.8	1.0

# Flow around a cylinder with triangular section $Re=1000$

## Vorticity fields and forces



# Conclusions

1. Chorin's approaches for solving NSEs in  $(\omega - u)$  and  $(u - p)$  were presented
  - ▶ A meshless Particle Vortex Method based on operator splitting and a mesh-based FVM based on pseudo - compressibility
2. The numerical behaviour of DVH was investigated for three geometries
  - ▶ All test cases were unsteady characterized by flow separation and shear layer formation
3. First two geometries: the simulations are accurate, capturing the separation point and the flow characteristics for increasing Re. Third case: sharp edges freeze the separation point and boundary singularities induce strong, localized gradients.
4. For each test case the convergence rates were studied for increasing Re
  - ▶ For smooth boundaries the rate degrades with increasing Re but is always at least 2 for both solvers
  - ▶ For non-smooth boundary the rate is  $O(1)$  for both solvers
5. Comparison with FVM - Pseudo Compressibility
  - ▶ Matching of the solutions in both local and global forces
  - ▶ Differences only for high Re for flow past a triangle, in the vortex positions in the far wake (different far wake resolution, transition to chaotic flow behaviour)

1. Chorin's approaches for solving NSEs in  $(\omega - u)$  and  $(u - p)$  were presented
  - ▶ A meshless Particle Vortex Method based on operator splitting and a mesh-based FVM based on pseudo - compressibility
2. The numerical behaviour of DVH was investigated for three geometries
  - ▶ All test cases were unsteady characterized by flow separation and shear layer formation
3. First two geometries: the simulations are accurate, capturing the separation point and the flow characteristics for increasing Re. Third case: sharp edges freeze the separation point and boundary singularities induce strong, localized gradients.
4. For each test case the convergence rates were studied for increasing Re
  - ▶ For smooth boundaries the rate degrades with increasing Re but is always at least 2 for both solvers
  - ▶ For non-smooth boundary the rate is  $O(1)$  for both solvers
5. Comparison with FVM - Pseudo Compressibility
  - ▶ Matching of the solutions in both local and global forces
  - ▶ Differences only for high Re for flow past a triangle, in the vortex positions in the far wake (different far wake resolution, transition to chaotic flow behaviour)

Giannopoulou O., Colagrossi A., Di Mascio A., Mascia C.: *Chorin's approaches revisited: Particle Vortex Method vs Finite Volume Method*, **submitted** to Engineering Analysis with Boundary Elements

1. Chorin's approaches for solving NSEs in  $(\omega - u)$  and  $(u - p)$  were presented
  - ▶ A meshless Particle Vortex Method based on operator splitting and a mesh-based FVM based on pseudo - compressibility
2. The numerical behaviour of DVH was investigated for three geometries
  - ▶ All test cases were unsteady characterized by flow separation and shear layer formation
3. First two geometries: the simulations are accurate, capturing the separation point and the flow characteristics for increasing Re. Third case: sharp edges freeze the separation point and boundary singularities induce strong, localized gradients.
4. For each test case the convergence rates were studied for increasing Re
  - ▶ For smooth boundaries the rate degrades with increasing Re but is always at least 2 for both solvers
  - ▶ For non-smooth boundary the rate is  $O(1)$  for both solvers
5. Comparison with FVM - Pseudo Compressibility
  - ▶ Matching of the solutions in both local and global forces
  - ▶ Differences only for high Re for flow past a triangle, in the vortex positions in the far wake (different far wake resolution, transition to chaotic flow behaviour)

Giannopoulou O., Colagrossi A., Di Mascio A., Mascia C.: *Chorin's approaches revisited: Particle Vortex Method vs Finite Volume Method*, **submitted** to Engineering Analysis with Boundary Elements

Thank you for your attention!